PHYSICAL REVIEW C VOLUME 47, NUMBER 4 APRIL 1993

ARTICLES

Forward angle analyzing power in $\vec{p}$-n and $\vec{p}$-p quasifree scattering at 643 and 797 MeV

G. Glass, T. S. Bhatia,* J. C. Hiebert, R. A. Kenefick, S. Nath,* L. C. Northcliffe, and W. B. Tippens†
Texas A&M University, College Station, Texas 77843

J. E. Simmons
Los Alamos National Laboratory, Los Alamos, New Mexico 87545

(Received 14 September 1992)

Polarized proton beams and a liquid-deuterium target were used to measure the analyzing power for quasifree $\vec{p}$-n and $\vec{p}$-p scattering in the forward direction at 643 and 797 MeV. Alternate use of a liquid-hydrogen target provided a comparison of free and quasifree $\vec{p}$-p scattering. The precision of the data is in general ±0.01 to ±0.02, although some of the $\vec{p}$-p data for 797 MeV are at the precision level of ±0.005. For c.m. angles $\theta^* \geq 22°$ there is no difference between quasifree and free results at either energy. The data are compared with the predictions of several phase-shift analyses. In a search for more pronounced quasifree scattering effects, a small amount of $\vec{p}$-"p" data were taken with a carbon target.

PACS number(s): 13.75.Cs, 21.30.+y, 24.70.+s

I. INTRODUCTION

The nucleon-nucleon (*NN*) scattering amplitudes at small forward angles have not been adequately determined despite numerous measurements available for both *n*-*p* and *p*-*p* scattering [1]. The small-angle scattering region is especially important for attempts to calculate nucleon-nucleus scattering in terms of multiple nucleon-nucleon interactions [2]. Data for both forward and backward angle *n*-*p* scattering will help to determine these forward amplitudes better. Many measurements, both quasifree (QF) and free, have been made in this energy and angle region [3–18], but often are inadequate due to uncertainties in normalization. The data presented here confirm much of the existing data with improved precision. Due to the intrinsic symmetry associated with pure isospin amplitudes, the full angular range of the $I=0$ amplitudes can be ascertained from the *p*-*p* (pure $I=1$) data and the charge-exchange *n*-*p* data. Three *I*-spin amplitude combinations contribute to *n*-*p* scattering: pure $I=1$, pure $I=0$, and interference of $I=1$ and 0. The pure $I=1$ amplitude contribution is obtained from *p*-*p* scattering, in which the product of cross section and analyzing power is necessarily antisymmetric about 90°. Another contribution to the antisymmetric part also comes from the pure $I=0$ amplitudes. The symmetric part is entirely made up of the interference of $I=1$ and 0 amplitudes. In order to determine this interference, it is essential that measurements of considerable precision be available for both the forward and the backward charge-exchange (CE) regions. The measurements reported here are of the analyzing power *A* for *p*-"*n*" QF scattering (where the "*n*" indicates that the neutron is bound in a nucleus, usually deuterium) for c.m. angles θ^* between 25° and 90° at 643 and 797 MeV. Measurements of the *A* values for free *p*-*p* and QF *p*-"*p*" scattering are also presented in order to show the negligibility of the effect produced by Fermi motion and the presence of a spectator nucleon in the deuterium nucleus.

II. EXPERIMENTAL METHOD AND APPARATUS

The polarized proton beam provided by the Clinton P. Anderson Meson Physics Facility (LAMPF) produced interactions in one of three interchangeable targets contained in a common vacuum chamber. The three target cells were identical, one being filled with liquid deuterium (LD_2), a second being filled with liquid hydrogen (LH_2), and the third (dummy cell) left empty. Each cell was a very short cylinder, of length 0.5 cm and diameter 4 cm, which was coaxial with the beam when in place. When pressurized to ~12 psi, the cell bulged to an axial length of ~0.9 cm in the beam direction. The target cell and vacuum windows were made of mylar of thickness 0.13 mm. After passage through the target, the transmitted proton beam was dumped ~7 m downstream of the target in a concrete-block array. The scattered proton and recoil proton or neutron were detected in a double-arm system shown in Fig. 1. The scattered proton was detected in the left arm, a spectrometer containing a dipole magnet M3 of C configuration, open on the beam side. The recoil proton or neutron was detected in the right arm. The layout shows the two arms near the symmetric $\theta_{\rm lab}=40°$ position corresponding to $\theta^*=90°$ for *N*-*N*

---

*Present address: AT Division, Los Alamos National Laboratory, Los Alamos, NM 87545.

†Present address: Physics Department, University of California, Los Angeles, CA 90024.

scattering. Shown also are a beamline deflection magnet M0, beam-focusing quadrupole magnets M1 and M2, an ion chamber IC, and two polarimeters, POL-A and POL-B.

The spectrometer arm contained two pairs of multiwire proportional chambers (MWPC's) (W1–W4), in front of and behind M3. The magnet aperture was ~40 cm horizontally by ~15 cm vertically, which provided a fairly uniform magnetic-field line integral up to about 15 kG m. The separation of the front pair of chambers was 86 cm and that of the back pair was 100 cm. Scintillators S1 and S2 (of thickness 1.6 and 6.4 mm, respectively) gave time-of-flight information over a 3.8-m path, which was used to distinguish protons from other particles (deuterons and pions) in the spectrometer. When multiple-scattering effects are included, the resolution was ~1% in momentum and ~0.25° in angle. A more detailed description of the spectrometer can be found in an earlier paper [19].

The recoil arm was designed to detect both neutrons and charged particles. It contained two MWPC's, W5 and W6, two large scintillator planes *R* and *V*, of thickness 6.4 mm, and a scintillator hodoscope neutron bar counter (NBC). The planes *R* and *V* are made from adjacent scintillator paddles (three for *R* and four for *V*), each of height 100 cm and width 23 cm.

The NBC was an array of 18 vertical scintillator bars, each of height 100 cm, width 7 cm and thickness 10 cm, arranged in a double row to form two layers of nine counters each. The total scintillator thickness of 20 cm provided neutron detection efficiencies between 10% and 20%. Each bar was optically isolated from the others, and a tag from its signal provided a horizontal coordinate, with resolution comparable to the width of the bar (7 cm). Photomultiplier tubes coupled to the top and bottom of each bar gave timing information; the time difference of the two signals was translated into a vertical location of accuracy ~7 cm for the event, and the time average provided a good signal for a time-of-flight measurement.

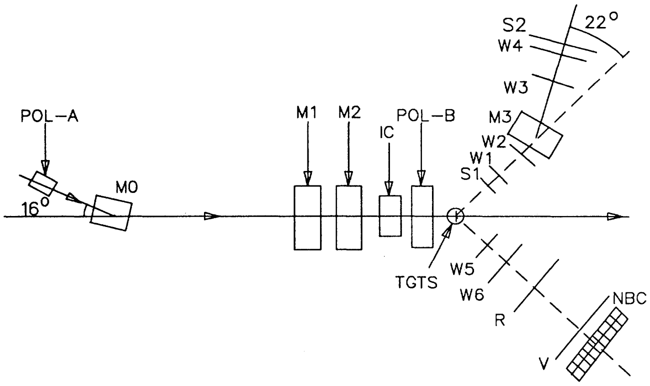

FIG. 1. Schematic diagram of the experimental setup. Labeling: POL-A and POL-B are polarimeters; M0 is a beam-line deflection magnet; M1 and M2 are beam-focusing quadrupole magnets; IC is an ion chamber. The target chamber (TGT) contains three interchangeable cells, one filled with LD_2, one with LH_2, and an empty "dummy" cell. The scattered protons are detected in the spectrometer arm, consisting of a spectrometer magnet M0, thin scintillators *S*1 and *S*2, and MWPC's W1–W4. The recoil protons and neutrons from free *p*-*p* and quasifree (QF) *p*-"*p*" and *p*-"*n*" scattering are detected in the recoil arm, which contained MWPC's W5 and W6, thin scintillator planes, *R* and *V*, and the scintillator hodoscope NBC (neutron bar counter). The recoil particle was identified as a neutron by the presence of a signal from the NBC accompanied by the absence of a signal from the veto counter *V*.

A charged particle in this arm was indicated by additional coincident signals from chambers W5, W6, and the two large thin scintillator planes, *R* and *V* (*pp* trigger). The absence of a signal from the veto encounter *V* coincident with a response from the NBC indicated (with certainty ≥99%) that the particle was neutral (*pn* trigger). Specifically, these triggers were defined as

$$pn = \mathrm{S1}\cdot\mathrm{S2}\cdot(\mathrm{W1}\cdot\mathrm{W2})_{3/4}\cdot(\mathrm{W3}\cdot\mathrm{W4})_{3/4}\cdot\mathrm{NBC}_{\mathrm{OR}}\cdot\bar{V}\ ,$$

$$pp = \mathrm{S1}\cdot\mathrm{S2}\cdot(\mathrm{W1}\cdot W2)_{3/4}\cdot(\mathrm{W3}\cdot\mathrm{W4})_{3/4}\cdot R\cdot(\mathrm{W5}\cdot\mathrm{W6})_{3/4}\ ,$$

or

$$pn = \mathrm{S1}\cdot\mathrm{S2}\cdot(\mathrm{W1}\cdot\mathrm{W2})_{3/4}\cdot(\mathrm{W3}\cdot\mathrm{W4})_{3/4}\cdot\mathrm{NBC}_{\mathrm{OR}}\cdot V\ ,$$

where the subscript 3/4 signifies a requirement of signals from at least three of the four MWPC planes and the subscript OR indicates the requirement of a signal from one or more of the individual bars of the NBC. The LH_2 target was used primarily with the *pp* trigger, but also was used to obtain background information for the *pn* trigger, as was the dummy target. These backgrounds were typically around 5–8 % and were easily separated from the primary signal, which appeared as a distinct peak in a histogram reflecting the "coplanarity" of the incident, scattered, and recoil particle paths. An example of such a histogram is shown in Fig. 2. During the LD_2 runs, hydrogen in the target cell walls contaminated the quasifree *p*-*p* data, since these events also were peaked in the coplanarity histograms. This contamination is observable in the shape of the coplanarity distribution (see Fig. 2) and was estimated to be less than 10%. Since the

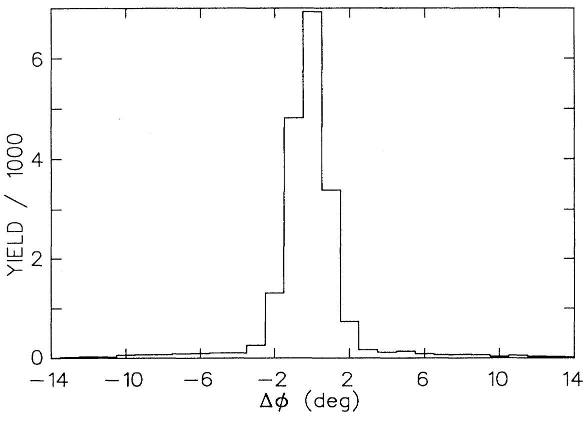

FIG. 2. Typical "coplanarity" histogram showing the angular deviation $\Delta\phi$ of the recoil particle from the scattering plane, which is defined by the paths of the incident and scattered protons.

differences observed between the quasifree and free values of the *p-p* data were less than 10%, this contamination affected the measured (uncorrected) values by only 1%, which is considerably less than the statistical errors.

The polarized beam intensity was monitored by an ion chamber IC just upstream of POL-B. The ion chamber was insensitive to polarization effects and therefore served as a reliable monitor of the relative intensity of the beam. In POL-B, both left-right and up-down asymmetries in *p-p* scattering from a thin (1.6-mm) CH_2 target were measured. It was found that the sum of the "up" and "down" scatterings observed in the polarimeter tracked very well (within 2%) with yields shown by the ion chamber and therefore could also be used as a relative intensity monitor. Beam intensities were in the range 1–6 pA, keeping dead-time and chance rates well below 10%.

The polarization of the proton beam was reversed at the ion source at intervals of ~2 min. The absolute polarization of the protons was measured at the ion source by the quench ratio method [8]; this technique is based on the atomic physics in the source and involves measurement of the ratio of beam intensities of "quenched" (essentially unpolarized) and "unquenched" beams. The measurement was made at the time during which the polarization was being reversed. When averaged over many cycles of polarization reversal, these measurements gave the absolute polarization of the beam in both its "up" and "down" orientations. This in turn permitted an absolute calibration of the analyzing power of POL-A to an accuracy of ±2%, thus giving an accurate absolute normalization of the *N-N* analyzing powers being measured. This is of special interest in the overlap region $60 \leq \theta^* \leq 90°$, where both forward angle measurements and CE measurements (made with a polarized target) [6] can be compared. This serves as a means of determining the target polarization in the latter experiment with greater absolute accuracy than could be achieved in the experiment itself, and could be used as a basis for renormalization of the CE measurements.

The systematic error is caused primarily by an uncertainty of 0.5° in the angle and is greatest in the region of zero crossing. Although not actually an error in the value of the analyzing power, it can be treated as such for the purpose of phase-shift analysis. For the *n-p* data this error is equivalent to 0.007 in the c.m. angular regions 10°–20° and 50°–100°. In all other regions the error is negligible when compared with the statistical error. For the *p-p* data this error is equivalent to 0.008 in the c.m. angular region 10°–30°, 0.003 between 40° and 60°, and 0.007 between 60° and 100°. Elsewhere it is negligible. The error is a point-to-point error and should be added in quadrature to the statistical error for insertion into a phase-shift analysis database. The data have been resubmitted to the SAID [2] database with this alteration of the errors.

III. RESULTS AND DISCUSSION

The *A* values measured for QF *p*-"*n*" scattering are presented in Table I, while Table II contains those measured for free *p-p* and QF *p*-"*p*" scattering, including a few results for QF *p*-carbon scattering at 797 MeV. The errors quoted for the *p-p* data are the statistical uncertainties of the two-arm detector data combined in quadrature with the statistical uncertainties of the beam-line polarimeter measurements; the latter were comparable to the former. The results are presented graphically, and compared with PSA predictions and data from other experiments, in Figs. 3–6.

In Fig. 3, the QF *p*-"*n*" analyzer power results from this experiment at 797 MeV are compared with those of Barlett *et al.* [3] and Bystricky *et al.* [4] at 800 MeV as well as with various free *n-p* measurements at nearby energies [5–7], and with various PSA predictions [20–22]. For angles below 50°, the *A* values obtained in this experiment are in excellent agreement with those obtained by Barlett *et al.* [3] and Bystricky *et al.* [4], and generally

TABLE I. Quasifree *p*-"*n*" analyzing power results.

θ^* (deg)	A	θ^* (deg)	A	θ^* (deg)	A
		$T_0=797$ MeV			
13.93	0.244±0.019	41.13	0.303±0.007	67.43	0.093±0.014
18.95	0.301±0.009	45.39	0.294±0.008	70.52	0.047±0.018
23.80	0.322±0.009	45.97	0.280±0.013	74.42	−0.002±0.009
26.91	0.314±0.010	50.19	0.255±0.008	79.28	−0.066±0.014
31.67	0.326±0.007	54.88	0.220±0.011	85.54	−0.212±0.031
36.51	0.336±0.009	59.63	0.184±0.018	89.38	−0.246±0.016
37.16	0.311±0.009	63.15	0.141±0.011	94.50	−0.225±0.027
		$T_0=643$ MeV			
14.68	0.268±0.019	40.08	0.297±0.014	66.89	0.102±0.016
18.85	0.309±0.012	44.76	0.294±0.010	68.28	0.024±0.033
22.69	0.298±0.008	47.34	0.255±0.020	72.21	0.006±0.015
25.85	0.353±0.018	51.19	).226±0.013	77.08	−0.061±0.020
29.47	0.328±0.010	55.54	0.209±0.016	87.07	−0.182±0.030
34.28	0.332±0.007	58.23	0.194±0.022	90.13	−0.263±0.020
35.66	0.282±0.023	62.20	0.136±0.012	94.50	−0.349±0.030

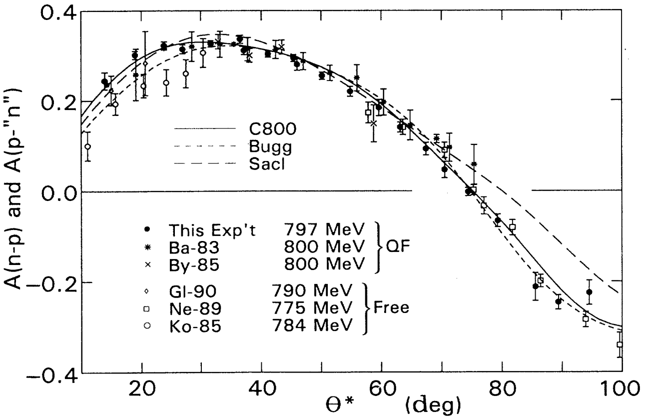

FIG. 3. Comparison of the quasifree (QF) *p*-"*n*" analyzing power results of the present experiment at 797 MeV with those of Ba-83 (Barlett *et al.* [3]) and By-85 (Bystricky *et al.* [4]) at 800 MeV, and with "free" *n*-*p* analyzing power results from Gl-90 (Glass *et al.* [5]), Ne-89 (Newsom *et al.* [6]), and Ko-85 (Korolev *et al.* [7]) at nearby energies. Also shown are the PSA predictions of Bugg [21], Bystricky *et al.* (SACL) [22], and the 800-MeV single-energy solution C800 of Arndt *et al.* [20].

have better statistical accuracy than either of the latter measurements. An exception occurs for three of the points of Ref. [3] (those at 14.3°, 23.8°, and 35.5°) which were assigned extremely small errors (0.001–0.002). These points very strongly influence the PSA fits. In fact, the VPI solution C800 [20] seems to be constrained to go through these three points. In a recent critical analysis of the *N*-*N* database [23], however, it is judged that these errors are unrealistic, and that they should be increased by adding 0.01 to them in quadrature, which would make them $\simeq 0.01$. This is comparable to the accuracy of the points of this experiment in the same angular region. For angles above 50°, the *A* values of the Barlett *et al.* deviate systematically, on the high side from those of this experiment, while the point at 59° from Bystricky *et al.* falls on the low side; these deviations are within or almost within the combined error bars of the experiments. As for comparison with the free *n*-*p* measurements, those of Glass *et al.* [5] at small angles are in acceptable agreement with the QF results, although somewhat lower systematically, and at larger angles the free scattering results of Newsom *et al.* [6] are in fairly good agreement with the present results (if the aberrant point at 95° is overlooked). On the other hand, there is strong disagreement between the free *n*-*p* measurements of Korolev *et al.* [7] and the QF data. The fact that the QF results are *higher* than the free results is contrary to expectations, since the multibody effects occurring in QF scattering would be more likely to decrease rather than enhance the observed analyzing power (as will be made more clear in the discussion of Fig. 4). The PSA fits were made without the benefit of the data of this experiment. The VPI fit [20] is dominated by the data of Barlett *et al.* at small angles and the data of Newsom *et al.* at large angles. The fit of Bugg [21] apparently is influenced much more by the data of Korolev *et al.* Apparently, the data of Newsom *et al.* were not included in the database for the Saclay fit [22] and its large-angle behavior is strongly influenced by the larger-angle data of Barlett *et al.* [3]. It deviates considerably from the results of this experiment and those obtained by Newsom *et al.* In part, the differences in

TABLE II. Free and quasifree *p*-*p* and *p*-"*p*" analyzing power results.

free (*p*-*p*)		quasifree (*p*-C)		quasifree (*p*-*d*)	
θ^* (deg)	*A*	θ^* (deg)	*A*	θ^* (deg)	*A*
		$T_0 = 797$ MeV			
18.90	0.368±0.023	37.15	0.363±0.024	18.24	0.355±0.027
22.11	0.411±0.007	41.17	0.382±0.015	21.92	0.406±0.011
25.22	0.444±0.011	45.80	0.380±0.015	25.03	0.444±0.015
31.65	0.461±0.005	51.90	0.366±0.023	32.28	0.461±0.007
41.48	0.498±0.008	64.20	0.299±0.024	41.86	0.497±0.008
51.02	0.482±0.005	75.58	0.290±0.031	51.44	0.483±0.006
63.15	0.412±0.013			63.15	0.420±0.015
74.21	0.298±0.015			74.21	0.282±0.011
		$T_0 = 643$ MeV			
27.3	0.517±0.009			28.8	0.474±0.012
33.3	0.555±0.008			33.8	0.531±0.009
38.8	0.533±0.020			38.7	0.537±0.014
44.2	0.549±0.016			44.4	0.527±0.012
60.5	0.449±0.020			49.0	0.513±0.026
66.4	0.365±0.017			54.7	0.504±0.019
70.8	0.278±0.023			60.7	0.385±0.025
76.3	0.243±0.019			66.4	0.355±0.021
87.3	0.034±0.031			71.0	0.319±0.028
92.4	−0.017±0.023			76.5	0.286±0.022
				87.2	0.072±0.031
				92.9	−0.013±0.022

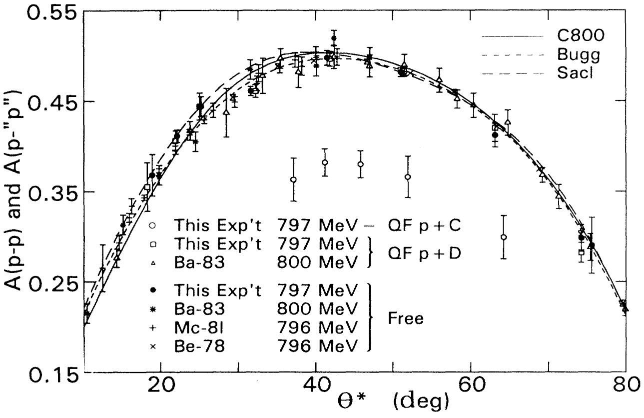

FIG. 4. Comparison of the quasifree p-"p" and free p-p analyzing power results of the present experiment at 797 MeV with the quasifree and free results of Ba-83 (Barlett *et al.* [3]), and with the free data of Mc-81 (McNaughton *et al.* [8]) and Be-78 (Bevington *et al.* [9]). Identification of the PSA predictions is the same as in Fig. 3. Also shown are a few points, obtained in this experiment, for QF p-"p" scattering from a carbon target. Small-angle ($\theta^* \leq 15°$) of Irom *et al.* [10] and Pauletta *et al.* [11] have been omitted from this plot because of the lack of overlap with the data of this experiment. A set of data at angles between 40° and 80° by Bystricky *et al.* [12] have also been omitted so as to avoid overclutttering the graph. The omitted data have somewhat larger error bars but tend to follow the same trend as the plotted points.

these PSA fits are due to differences in the database used in each analysis and the relative weightings assigned to the data, but some differences are also attributable to the way inelasticities are handled in each analysis [24]. The data of the present experiment follow the VPI curve most closely but tend to fall slightly below the curve for angles above 40°.

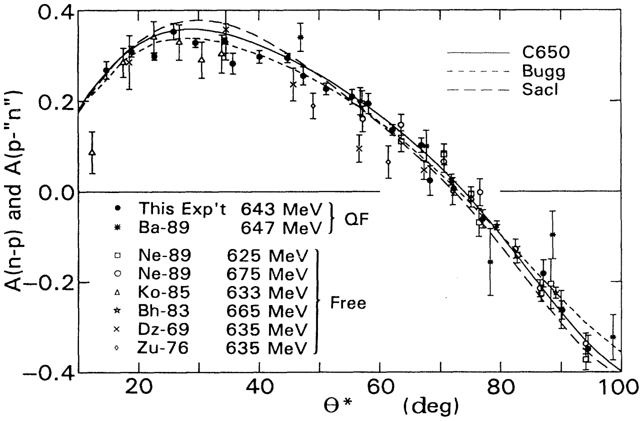

FIG. 5. Comparison of the quasifree p-"n" analyzing power results of the present experiment at 643 MeV with those of Ba-89 (Bartlett *et al.* [3]). Also shown are free n-p results from Ne-89 (Newsom *et al* [6]), Ko-85 (Korelev *et al.* [7]), Bh-83 (Bhatia *et al.* [13]), Dz-64 (Dzhelepov *et al.* [14]), and Zu-76 (Zulkarneev, Murtazaev, and Khachaturov [15]). The PSA predictions are as identified in Fig. 3, except that the VPI curve is the single energy solution C650.

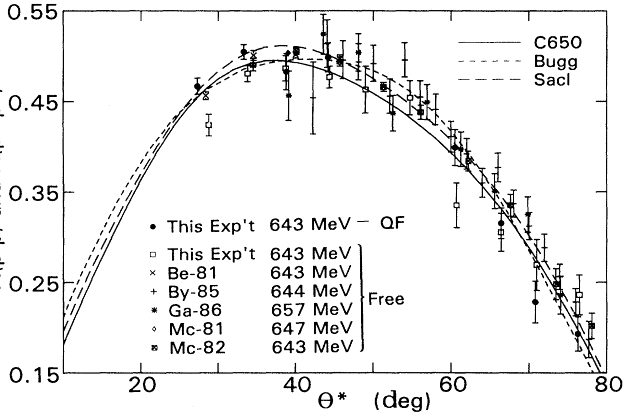

FIG. 6. Comparison of the quasifree p-"p" and free p-p analyzing power results of the present experiment at 643 MeV with the free p-p results of Be-81 (Bevington *et al.* [9]), By-85 (Bystricky *et al.* [12]), Ga-87 (Garçon *et al.* [16]), Mc-82 (McNaughton *et al.* [17]), and Mc-81 (McNaughton and Chamberlin [18]). The PSA predictions are as identified in Fig. 5.

A more direct determination of the effect QF scattering has on the analyzer power is possible in the case of p-p scattering, in which the results obtained with a free-nucleon target (LH_2) can be compared with those obtained with a bound-nucleon target (LD_2). The results of numerous experiments [3,8,9] in the vicinity of 800 meV are shown in Fig. 4. The overall agreement is very good. In two of these experiments, the present one and that of Barlett *et al.* [3], both free and QF scattering (from a deuterium target) were measured with the same apparatus. A detailed examination of these results reveals no significant systematic difference between the A values for free and QF scattering. The Fermi motion of the target proton and the presence of a loosely bound spectator neutron in the deuterium target apparently has no measurable effect on the analyzing power. Such is not the case, however, when the target proton is more tightly bound in a heavier nucleus, as is shown by the A values obtained for QF p-"p" scattering with a carbon target, also displayed in Fig. 4. The values of A are reduced substantially. In fact, even larger reductions in the A values for QF p-C scattering relative to those for free p-p scattering have been observed at other energies [25]. An attempt to explain the large decrease in analyzing power by averaging over the Fermi motion of the target proton was unsuccessful. Presumably, plural strong interactions with the nucleons in such a target cause depolarization of the incoming and outgoing protons, the net effect of which is to decrease the analyzing power. The fact that the depolarization parameters are large for small-angle N-N scattering lends plausibility to this explanation. The PSA fits in this case differ very little, but on the whole, the fit of Bugg seems to be best.

The A values obtained for p-"n" QF scattering at 643 MeV in this experiment are compared in Fig. 5 with the QF data of Barlett *et al.* [3] at 647 MeV and the free n-p scattering results of several other experiments at nearby energies [6,7,13–15] and the PSA fits. Here the agreement is not quite as good, but if the older data of Dzhelepov [14] and Zulkarneev, Martazaev, and Khachaturov [15] and the statistically less accurate data of Barlett *et al.* [3] are excluded, the picture does not look too bad. At this energy there is no significant disagreement with the results of Korolev *et al.* [7] beyond the rather large statistical errors of the latter data, which tends to substantiate the argument that the disagreement seen at 800 meV is not a real effect but rather the result of some sort of experimental error. With regard to the remaining data, there is relatively good agreement with the free-scattering results of Newsom *et al.* [6] and Bhatia *et al.* [13]. Once again, no systematic difference between the free and QF results is evident. It is worth noting that the data of this experiment, at least at smaller angles, are more plentiful and statistically more precise than the earlier results. Unfortunately, some fluctuations are seen which are outside the statistical precision. Again, the differences between the PSA fits are small, but the VPI fit [20] seems to be best for the largest angles and the fit of Bugg [21] seems to be better at the smaller angles.

The picture is rounded out by Fig. 6, which shows the free *p-p* and QF *p*-"*p*" results of this experiment at 643 MeV in comparison with various free *p-p* data in the same energy region [9,12,16–18]. Here there appears to be a difference between the free and QF results of this experiment for angles below 40°. In view of the equality found for analogous data in Figs. 3–5, it is suspected that this effect is not real, but rather the result of experimental error. The addition of the systematic error mentioned in Sec. II to the free and quasifree points would put this discrepancy at the level of about 2.5 standard deviations. It is difficult to believe that there would be so large a difference between the *A* values for free and QF scattering for such large angles at 643 MeV when no difference is found at 790 MeV for angles as small as 22°. The momentum transfer for 29° at 643 MeV, for example, is the same as that for 26° at 797 MeV. One would expect from Glauber theory [26] that the effect of screening would be about the same at the same momentum transfer. The four-momentum-transfer squared is near 0.07 $(\mathrm{GeV}/c)^2$ in this scattering region, which corresponds to distances less than 10^{-13} cm, considerably smaller than the size of the deuteron ($>3\times10^{-13}$ cm). Thus, the effects of screening are not expected to be significant. A clue as to the cause of the discrepancy lies in the beam-polarization determination, which can be found alternatively from the quench-ratio measurements or the asymmetry measured in POL-A. These were found to be inconsistent for the points in question, in opposite senses for the free and QF measurements, and could account for the discrepancies.

IV. CONCLUSIONS

The new analyzing-power measurements presented here cover a significant region for forward *p*-"*n*" QF scattering from deuterium at two energies. They span a wider angular range and are of precision comparable to or better than that of previous QF measurements at about the same two energies [3,4]. When compared with the *A* values measured in previous free *n-p* scattering experiments [5–7,13–15], no significant systematic difference is found for the angular region of overlap, the precision of the data is comparable to or better than that of the free *p-p* data, and the angular range spanned is broadened considerably. In an essentially simultaneous measurement of the *A* value for QF *p*-"*p*" and free *p-p* scattering with the same apparatus, again, no significant systematic difference is seen, in this experiment or in comparison with other available free *p-p* analyzing power measurements [3,8,9,16–18]. This lack of difference between QF and free scattering in the four-momentum-transfer region ≥ 250 MeV/*c* should be calculable within the framework of Glauber screening [26]. The results presented here can be added to the analyzing power database, broadening it considerably, making possible a better determination of the $I=0$ phase shifts and forward-scattering amplitudes, which are very important for an understanding of *N*-nucleus scattering. A few QF *p*-"*p*" data obtained with a carbon target at 797 MeV show that *A* is considerably reduced when the target is a nucleus heavier than deuterium.

ACKNOWLEDGMENTS

We are grateful to the LAMPF operations staff for providing us with steady highly polarized beam, and to the cryogenics group led by J. Novak for producing a problem-free triple target. This work was supported in part by the U.S. Department of Energy under Contract No. DE-AS05-ER04449 and Grant No. DE-FG05-88ER40399.

---

[1] R. A. Arndt, Phys. Rev. D **37**, 2665 (1988).
[2] J. Bystricky, C. Lechanoine-Leluc, and F. Lehar, J. Phys. (Paris) **48**, 199 (1987); G. W. Hoffmann, private communication.
[3] M. L. Barlett *et al.*, Phys. Rev. C **27**, 682 (1983); **40**, 2697 (1989).
[4] J. Bystricky *et al.*, Nucl. Phys. A **444**, 597 (1985).
[5] G. Glass *et al.*, Phys. Rev. C **41**, 2732 (1990).
[6] C. R. Newsom *et al.*, Phys. Rev. C **39**, 965 (1989).
[7] G. A. Korolev, A. V. Khanzadeev, G. E. Petrov, E. M. Spiridenkov, A. A. Vorobyov, Y. Terrien, J. C. Logul, J. Saudinos, B. H. Silverman, and F. Wellers, Phys. Lett. B **165**, 262 (1985).
[8] M. W. McNaughton, P. R. Bevington, H. B. Willard, E. Winkelmann, E. P. Chamberlin, F. H. Cverna, N. S. P. King, and H. Willmes, Phys. Rev. C **23**, 1128 (1981).
[9] P. R. Bevington *et al.*, Phys. Rev. Lett. **41**, 384 (1978).
[10] F. Irom, G. J. Igo, J. B. McClelland, and C. A. Whitten, Jr., Phys. Rev. C **25**, 373 (1982).
[11] G. Pauletta, G. Adams, S. M. Haji-saeid, G. J. Igo, J. B. McClelland, A. T. M. Wang, C. A. Whitten, Jr., A. Wriekat, M. M. Gazzaly, and N. Tanaka, Phys. Rev. C **27**, 282 (1983).
[12] J. Bystricky *et al.*, Nucl. Phys. B **262**, 727 (1985).

[13] T. S. Bhatia *et al.*, in *Polarization Phenomena in Nuclear Physics-1980,* Proceedings of the Fifth International Symosium, Santa Fe, edited by G. G. Ohlsen, R. E. Brown, N. Jarmie, M. W. McNaughton, and G. M. Hale, AIP Conf. Proc. No. 69 (AIP, New York, 1981), p. 123, and in the SAID database of Ref. [1] (unpublished).

[14] V. P. Dzhelepov, in Proceedings of the XII International Conference, Dubna, 1964 (unpublished).

[15] R. Zulkarneev, K. H. Murtazaev, and V. Khachaturov, Phys. Lett. B **61**, 164 (1976).

[16] M. Garçon, J. C. Duchazeubeinex, J. C. Faivre, B. Guillerminet, D. LeGrand, M. Rouger, J. Saudinos, and J. Arvieux, Phys. Lett. B **183**, 273 (1987).

[17] M. W. McNaughton, E. P. Chamberlin, J. J. Jarmer, N. S. P. King, H. B. Willard, and E. Winkelman, Phys. Rev. C **25**, 2107 (1982).

[18] M. W. McNaughton and E. P. Chamberlin, Phys. Rev. C **24**, 1778 (1981).

[19] W. B. Tippens *et al.,* Phys. Rev. C **36**, 1413 (1987).

[20] R. A. Arndt, L. D. Roper, R. A. Bryan, R. B. Clark, B. J. VerWest, and P. Signell, Phys. Rev. D **28**, 97 (1983); R. A. Arndt, J. S. Hyslop III, and L. D. Roper, *ibid.* **35**, 128 (1987), and the VPI PSA and SAID program

[21] D. V. Bugg, Phys. Rev. C **41**, 2708 (1990), and the Bugg PSA.

[22] See the Saclay PSA in Ref. [2].

[23] R. A. Arndt, L. D. Roper, R. L. Workman, and M. W. McNaughton, Phys. Rev. D **45**, 3995 (1992).

[24] E. Lomon, private communication.

[25] J. Bystricky *et al.,* J. Phys. (Paris) Colloq. **46**, C2-483 (1985).

[26] R. J. Glauber, in *Proceedings of the International Conference on High Energy and Nuclear Structure,* Columbia University, New York, 1969, edited by S. Devins (Plenum, New York, 1970), p. 207.